Neocortex Network Activation and Deactivation States Controlled by the Thalamus

Akio Hirata and Manuel A. Castro-Alamancos

J Neurophysiol 103:1147-1157, 2010. First published 6 January 2010;
doi: 10.1152/jn.00955.2009

J Neurophysiol 103: 1147–1157, 2010.
First published January 6, 2010; doi:10.1152/jn.00955.2009.

Neocortex Network Activation and Deactivation States Controlled by the Thalamus

Akio Hirata and Manuel A. Castro-Alamancos
Department of Neurobiology and Anatomy, Drexel University College of Medicine, Philadelphia, Pennsylvania

Submitted 29 October 2009; accepted in final form 1 January 2010

Hirata A, Castro-Alamancos MA. Neocortex network activation and deactivation states controlled by the thalamus. *J Neurophysiol* 103: 1147–1157, 2010. First published January 6, 2010; doi:10.1152/jn.00955.2009. Neocortex network activity varies from a desynchronized or activated state typical of arousal to a synchronized or deactivated state typical of quiescence. Such changes are usually attributed to the effects of neuromodulators released in the neocortex by nonspecific activating systems originating in basal forebrain and brain stem reticular formation. As a result, the only role attributed to thalamocortical cells projecting to primary sensory areas, such as barrel cortex, is to transmit sensory information. However, thalamocortical cells can undergo significant changes in spontaneous tonic firing as a function of state, although the role of such variations is unknown. Here we show that the tonic firing level of thalamocortical cells, produced by cholinergic and noradrenergic stimulation of the somatosensory thalamus in urethane-anesthetized rats, controls neocortex activation and deactivation. Thus in addition to its well-known role in the relay of sensory information, the thalamus can control the state of neocortex activation, which may complement the established roles in this regard of basal forebrain and brain stem nuclei. Because of the topographical organization of primary thalamocortical pathways, this mechanism provides a means by which area-specific neocortical activation can occur, which may be useful for modality-specific sensory processing or selective attention.

INTRODUCTION

The main relay station to the neocortex is the thalamus (Castro-Alamancos and Connors 1997; Sherman and Guillery 1996; Steriade et al. 1997). Thalamocortical cells in the ventroposterior medial nucleus of the thalamus (VPM) provide the primary input to the somatosensory (barrel) cortex and their main role is to transmit sensory information from the periphery to the neocortex. In addition to their prominent role in sensory relay, VPM cells can undergo significant changes in spontaneous firing rate. A well-known transition is the change between bursting and tonic firing (Sherman and Guillery 1996; Steriade et al. 1997). Within the tonic mode, thalamocortical neurons in VPM, and in other modalities, vary considerably in their spontaneous firing rate, depending on behavioral state (Bezdudnaya et al. 2006; Castro-Alamancos 2002a,b; Castro-Alamancos and Oldford 2002; Guido and Weyand 1995). It is not known how changes in tonic thalamocortical firing of VPM neurons affect network activity in the barrel cortex where they project.

The network activity of the neocortex undergoes significant changes during different behavioral states. During arousal, vigilance and paradoxical sleep, neocortical spontaneous electrical activity consists of low-amplitude fast rhythms that appear to be asynchronous between neuronal populations—a state that is commonly termed *desynchronized* or *activated*. In contrast, during states of drowsiness or sleep, neocortical spontaneous activity consists of large-amplitude slow rhythms that are highly synchronized among neuronal populations—a state that is commonly termed *synchronized* or *deactivated* (for examples of these changes during chronic recordings in behaving rats see Castro-Alamancos 2004a, 2009; Castro-Alamancos and Oldford 2002). It has been known for some time that these cortical states are controlled by cells in the brain stem reticular formation (Moruzzi and Magoun 1949). In the brain stem, cholinergic neurons within the pontomesencephalic tegmentum in the laterodorsal (LDT) and pedunculopontine tegmental (PPT) nuclei project to the thalamus (Hallanger et al. 1987; Satoh and Fibiger 1986). Cholinergic neurons in the LDT/PPT complex discharge vigorously during paradoxical sleep and also during wakefulness (el Mansari et al. 1989; Steriade et al. 1990), and the levels of acetylcholine increase in the thalamus during those states (Williams et al. 1994). Noradrenergic fibers originating in the locus ceruleus (LC) within the brain stem also project to the thalamus (Lindvall et al. 1974) and LC neurons discharge robustly during high levels of vigilance and attention, reduce their firing during slow-wave sleep, and stop firing during paradoxical sleep (Aston-Jones and Bloom 1981; Foote et al. 1980; Hobson et al. 1975). We recently found that the spontaneous firing of VPM neurons is differentially influenced by cholinergic and noradrenergic actions in the thalamus (Hirata et al. 2006). Cholinergic thalamic activation sharply increases the spontaneous firing of VPM neurons, whereas noradrenergic thalamic activation robustly drives nucleus reticularis thalamic (nRt) firing and abolishes the spontaneous firing of VPM neurons.

In the present study, we tested the effect of cholinergic or noradrenergic activation of the somatosensory thalamus on the spontaneous network activity of barrel cortex neurons. We found that increases in spontaneous tonic firing of VPM neurons caused by cholinergic stimulation of the thalamus led to neocortical activation or desynchronization, whereas abolishment of VPM tonic firing caused by noradrenergic stimulation of the thalamus led to neocortical deactivation or synchronization. We conclude that thalamocortical tonic firing per se, which is regulated by brain stem neuromodulators, controls the state of neocortical activation.

METHODS

Surgery

Sprague–Dawley rats (300–350 g) were used in this study and cared for in accordance with National Institutes of Health guidelines

Address for reprint requests and other correspondence: M. Castro-Alamancos, Department of Neurobiology and Anatomy, Drexel University College of Medicine, 2900 Queen Lane, Philadelphia, PA 19129 (E-mail: mcastro@drexelmed.edu).

for laboratory animal welfare. All experiments were approved by the Drexel University Institutional Animal Care and Use Committee. Rats were anesthetized with urethane (1.5 g/kg, administered intraperitoneally) and placed in a stereotaxic frame. All skin incisions and frame contacts with the skin were injected with lidocaine (2%). A unilateral craniotomy extended over the parietal cortex. Small incisions were made in the dura as necessary. Body temperature was automatically maintained constant with a heating pad at 37°C. The level of anesthesia was monitored with field potential (FP) recordings and limb-withdrawal reflexes and kept constant at about stage III/3 using supplemental doses of urethane. In the present study this state is called the *control* state and consists of 0.5- to 10-Hz FP activity (with predominance of 2–4 Hz) and is also characterized by the absence of whisker movements and pinch withdrawal reflex.

Electrophysiology

In every experiment, a tungsten electrode (1–2 MΩ) was lowered into the depth of the barrel cortex (0.8–1 mm) contralateral to the stimulated whiskers to record FP and multiunit activity (MUA). FP polarity is plotted as negative down. MUA was measured by using a threshold detector to count the number of events. The threshold was adjusted off-line at the beginning of the experiment just above the noise level during down states and kept constant throughout the experiment. In addition, a single-unit (extracellular) or an intracellular electrode was lowered adjacent to the FP electrode (<300 μm horizontally) to record from cells located in layer 2/3 (200–700 μm in depth) and layer 4 (700–950 μm). To conduct single-unit recordings in the barrel cortex, a high-impedance (5–30 MΩ) glass electrode filled with artificial cerebrospinal fluid (ACSF) was used. These electrodes yield highly isolated single units; usually the spike from only one cell is present with a high signal to noise ratio. Single units were classified as fast spiking (FS) or regular spiking (RS), based on spike width, as previously described (Hirata and Castro-Alamancos 2008). RS cells had a spike width >0.3 ms and FS cells had a width <0.2 ms. FS cells had a spontaneous firing rate >2 Hz, whereas most RS cells generally had a spontaneous firing rate <1 Hz. However, a number of RS cells generally located in layer 4 present significantly higher spontaneous firing rates. The timing of single units was measured using interevent time histograms (IETHs), which measures the interval between successive spikes. The timing of MUA was measured using autocorrelations, which measures the interval between each detected spike and all the other spikes.

To conduct intracellular recordings in the barrel cortex, a high-impedance (80–120 MΩ) sharp electrode filled with K-acetate (2 M) was lowered into the vicinity of the FP electrode. All intracellular recordings included in the study had overshooting action potentials and a stable membrane potential (V_m) for >30 min. Intracellular recordings were usually done without any constant current (DC = 0 nA) or with a small amount of constant negative current (DC = −0.2 nA) to compensate for a potential leak caused by the impalement. Current pulses used to determine intrinsic firing and input resistance (R_{in}) were 500 ms in duration, delivered every 5–10 s. Input resistance was measured using negative current pulses (−0.3 nA). The voltage deflection used for the calculation was obtained by averaging the V_m between 100 and 150 ms after pulse onset. The final R_{in} value was obtained by averaging the results from multiple pulses delivered during 5–10 min of continuous recording in each state. Continuous periods of V_m recordings, excluding brief periods of current pulses or afferent stimulation, lasting 5–10 min in each state, were used to derive distributions of counts at each V_m (1-mV bin), which indicate the amount of time that the neuron spends at each V_m. These distributions were further analyzed by measuring the kurtosis or peakedness of the distribution and obtaining the peak V_m value by fitting each distribution with a nonlinear Gaussian function.

Microdialysis

To apply drugs into the somatosensory thalamus, a microdialysis cannula (outer diameter, 250 μm; membrane, 2 mm long) was placed around the following coordinates: posterior = 3, lateral = 2–3, depth = 4–6, as previously described (Aguilar and Castro-Alamancos 2005; Hirata et al. 2006). The cannula entered into the brain at an angle (~30°) from the midline and is inside VPM, which it traverses in a medial-to-lateral and dorsal-to-ventral direction (see Aguilar and Castro-Alamancos 2005 for a histological example). ACSF was continuously infused through the probe at 2–4 μl/min. ACSF contained (in mM): NaCl, 126; KCl, 3; NaH_2PO_4, 1.25; $NaHCO_3$, 26; $MgSO_4 \cdot 7H_2O$, 1.3; dextrose, 10; and $CaCl_2 \cdot 2H_2O$, 1. Norepinephrine (NE) and carbachol (CA) were used at 0.5–1 and 0.2–0.5 mM, respectively. These doses were previously shown to significantly affect the spontaneous firing and whisker-evoked responses of thalamic cells under the same conditions (Castro-Alamancos 2002a; Hirata et al. 2006). CA is not easily metabolized by cholinesterase and remains active for quite some time after application. Thus we made no effort to wash out the effect of CA. Instead, we directly substituted CA with NE in the medium as a way to immediately reverse the effects of CA. This rapidly changes the tonic firing of VPM cells from a high rate during CA to nil during NE (Hirata et al. 2006).

Based on experience and a typical exchange of about 10% (reverse dialysis recovery), the effective doses used during microdialysis are about 10-fold those used during direct application in slices (Castro-Alamancos 2002b; Castro-Alamancos and Calcagnotto 2001). Based on diffusion experiments using arrays of recording electrodes at different distances from the probe, we have estimated the spread of these drugs to be <1 mm in the horizontal plane away from the membrane (Aguilar and Castro-Alamancos 2005; Castro-Alamancos 2000; Hirata et al. 2006). This affects most of the somatosensory thalamus (Paxinos and Watson 1982) since it is centered in VPM and spreads anterior into nRt (as shown previously; Hirata et al. 2006) and posterior into the medial sector of the posterior nucleus (POm) of the thalamus. However, other thalamic nuclei, including intralaminar or midline nuclei, are too far to be affected by the diffusion. For simplicity, throughout this study we will refer to the thalamic diffusion site as VPM.

Data analysis

If the data were considered normally distributed, according to the Shapiro–Wilk normality test, we used parametric statistics; otherwise, we used nonparametric tests. In general, normally distributed data were first tested for a significant main effect using a repeated-measures ANOVA followed by multiple comparisons with Tukey's test. Nonparametric comparisons consisted of the Wilcoxon signed-ranks test.

Histology

At the end of the experiments, the animals were given an overdose of sodium pentobarbital and either perfused through the heart with saline followed by paraformaldehyde (4%) or the brain was directly extracted and placed in the fixative. The brains were then sectioned in the coronal plane using a vibratome (80–100 μm) and processed for Nissl staining to confirm the location of the microdialysis probe in the somatosensory thalamus (Hirata and Castro-Alamancos 2006).

RESULTS

Cortical activation and deactivation states produced by thalamic neuromodulators

Application of a cholinergic agonist in the thalamus (CA in VPM) significantly enhances the firing rate of VPM cells,

whereas subsequent application of NE (NE in VPM) immediately abolishes the firing of VPM cells (Hirata et al. 2006). We tested the effect of cholinergic and noradrenergic thalamic stimulation on cortical cells in the barrel cortex. First, we report the effects of these thalamic manipulations on the spontaneous FP, MUA, and single-unit cortical activity. Later, we report the effects on intracellular cortical activity.

During control conditions (see METHODS), FP, MUA, and single-unit recordings display spontaneous synchronous slow oscillations. Application of CA in VPM produces an immediate abolishment of this activity. Figure 1 shows examples from two different experiments. The traces in Fig. 1*A* show typical large-amplitude slow waves of the FP; the negative FP peaks are tightly synchronized with MUA recorded through the same electrode and with the firing of a simultaneously recorded layer 3 single unit (RS cell; 465 μm in depth) recorded from a nearby electrode. The periods of synchronous firing in the MUA during the slow oscillations correspond with intracellular up states (see following text). In between the negative FP peaks are periods of nil firing that can correspond with intracellular down states. During application of CA in VPM, the large waves of FP and MUA activity are abolished and the longer periods of nil MUA are not obvious. Moreover, the layer 3 cell in Fig. 1*A* significantly reduced its spontaneous firing. The changes in FP and MUA activity produced by CA in VPM resemble those traditionally termed *activation* or *desynchronization* (Moruzzi and Magoun 1949; Steriade et al. 1991), which occur when an animal transitions between a sleep/quiescent state to an awake/vigilance state.

Figure 1*B* shows another experiment from which several parameters were calculated continuously as drugs were infused into VPM. We measured the power spectrum of the FP activity during each second of continuous recording (FFT) and the number of spikes/s (Hz) of MUA (1-s bins). Application of CA

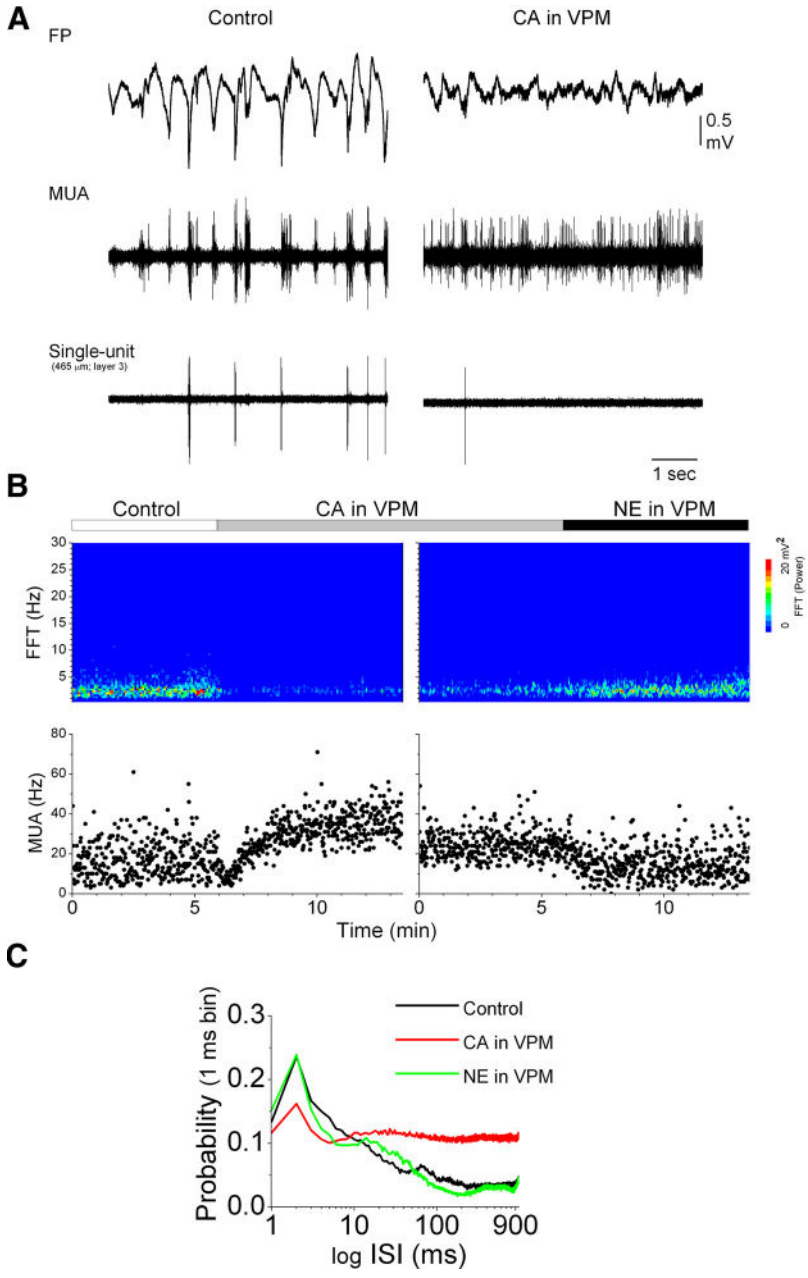

FIG. 1. Effects of thalamic neuromodulators on barrel cortex extracellular activity. *A*: field potential (FP), multiunit activity (MUA), and single-unit traces recorded in the barrel cortex during control and during application of carbachol (CA) in ventroposterior medial nucleus of the thalamus (VPM). *B*: quantification of the effects of CA in VPM and subsequent norepinephrine (NE) in VPM from an experiment different from that in *A*. The *top panel* shows a Fast Fourier Transform (FFT) power spectrum of the spontaneous FP activity measured continuously and displayed as a contour color plot. The *bottom panel* shows the number of events detected/s (Hz) in the MUA recording measured continuously. *C*: autocorrelation of the MUA for the experiment shown in *B* during control, CA in VPM, and NE in VPM.

in VPM abolished the low-frequency FP activity and eliminated the instances of nil MUA activity, indicating that down states typical of control conditions were abolished. Subsequent application of NE in VPM completely reversed the effects of CA in VPM. Thus the slow FP oscillations and the MUA down states (bins with near zero firing) were restored to a state similar to that of control conditions (Fig. 1*B*).

In addition, autocorrelation analysis of the MUA (Fig. 1*C*) showed a typical large-amplitude peak at high frequencies (>100 Hz) corresponding to the characteristic synchronous high-frequency population firing during control. During CA in VPM there was a reduction of high-frequency synchronous population firing (>100 Hz) and an increase in lower-frequency population firing (<50 Hz), so that the MUA autocorrelation was almost flat, and these effects were reversed by NE in VPM.

Figure 2 shows FP and MUA population data from several experiments ($n = 8$) in which CA in VPM was applied followed by NE in VPM. CA in VPM produced a significant reduction of low-frequency FP activity between 0.1 and 10 Hz ($P < 0.01$; Fig. 2*A*), but does not significantly affect higher frequencies (10–50 Hz; n.s.); this is reversed by subsequent application of NE in VPM ($P < 0.01$; Fig. 2*A*). CA in VPM produced a significant increase in MUA firing rate ($P < 0.01$; Fig. 2*B*), which was reversed by NE in VPM ($P < 0.01$; Fig. 2*B*). However, we emphasize that firing rates obtained from MUA must be considered carefully because during highly synchronous firing states (i.e., control in the present study) the spikes from multiple cells merge into a single population spike that obviously underestimates the actual firing rate. This is evident in Fig. 1*A* by comparing the larger peak amplitude MUA spikes during control compared with CA in VPM. Thus well-isolated single units (described in the following text) are a better measure of firing rates during the different conditions. The coefficient of variation (CV) of continuous MUA firing rate measurements (1-measure/s over a 5-min period for each condition; see Fig. 1*B*) revealed a significant reduction during CA in VPM ($P < 0.01$), which indicates that the measured firing rate is less variable during CA in VPM than that during control or NE in VPM (Fig. 2*C*). This is expected because of the continuous fluctuations between up (high firing) and down (nil firing) states during control and NE in VPM. Finally, Fig. 2*D* shows these changes reflected in the MUA autocorrelation. CA in VPM produced a significant reduction in high-frequency MUA firing probability (>50 Hz; $P < 0.01$) and a concomitant increase in low-frequency firing probability (1–5 Hz; $P < 0.01$).

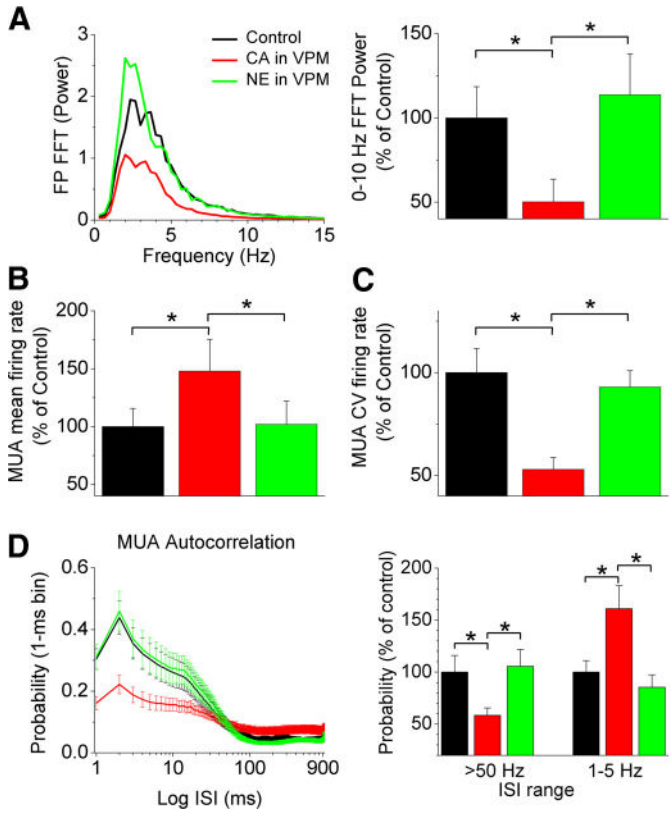

FIG. 2. Group data showing the effects of thalamic neuromodulators on population extracellular activity in barrel cortex. *A*: FFT power spectrum of FP activity during control, CA in VPM, and NE in VPM plotted as an FFT function (*left*) or integrated between 0 and 10 Hz (*right*). *B*: mean (*left*) and coefficient of variation (CV, *right*) of MUA firing rate during control, CA in VPM, and NE in VPM. *C*: average MUA autocorrelation (means ± SE) during the 3 conditions (*left*) and integrated for high frequencies (>50 Hz) or low frequencies (1–5 Hz). *$P < 0.01$.

For simplicity, we will term the effects just described of thalamic cholinergic stimulation on spontaneous cortical FP and MUA activity, *activation*, and those of thalamic noradrenergic stimulation, *deactivation*. It is also worth noting that, in a few experiments, we applied NE first (before CA) and found the same deactivating effect; e.g., the low-frequency power spectrum increased significantly compared with control (not shown). Since the VPM firing rate is very low (Hirata et al. 2006) and the cortex is mostly in a deactivated state during our control conditions, the deactivating effect of thalamic NE is most noticeable when compared with the activation produced by thalamic CA.

Behavior of FS cells is different from that of RS cells during activation and deactivation states

We recorded from well-isolated barrel cortex single units ($n = 19$) during control conditions, application of CA in VPM, and subsequent application of NE in VPM. Most of these cells were RS cells ($n = 15$) and a few were FS cells ($n = 4$), which are putative GABAergic interneurons. RS cells significantly reduced their firing rate during activation produced by application of CA in VPM; this was reversed by deactivation produced by NE in VPM ($P < 0.01$; Fig. 3*A*). The effect of activation on firing rate was somewhat dependent on the layer where the RS cell was located since there was a significant correlation between cell depth and the change in firing rate caused by CA in VPM (Fig. 3*B*). Thus whereas all layer 2/3 cells reduced their spontaneous firing rate during CA in VPM compared with control, just half of layer 4 cells reduced their firing rate whereas the other half slightly increased their firing rates (Fig. 3*B*). In contrast, FS cells behaved quite differently. We recorded from a few FS cells ($n = 4$) located in layer 4. All of these cells increased their firing rate rather significantly during activation produced by application of CA in VPM and this was reversed by NE in VPM ($P < 0.01$; Fig. 3C).

Figure 4 shows examples of the effects of CA in VPM and NE in VPM on FS cells. Figure 4*A* shows traces from an FS cell that was located in layer 4 (850 μm in depth), responded with a large high-frequency burst (>100 Hz) to whisker stimulation, and was exceedingly well coupled to thalamocortical cells because it could follow putative spontaneous tha-

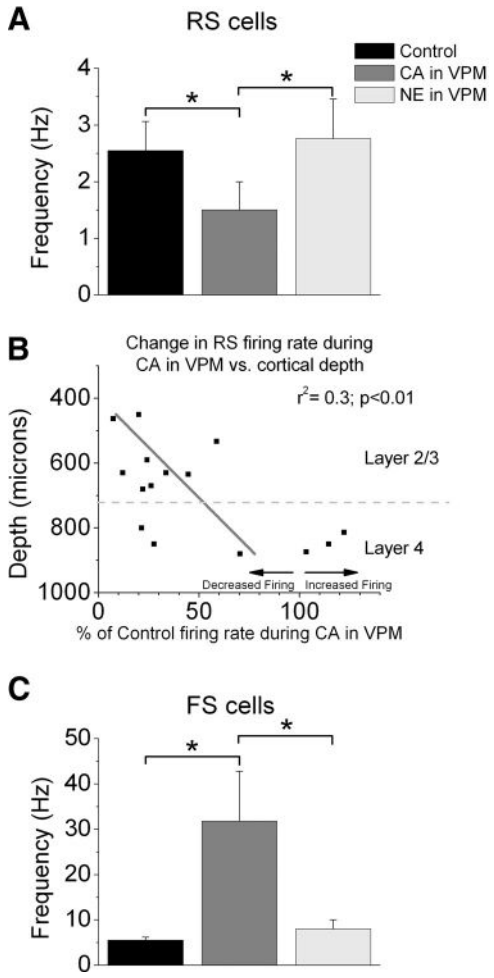

FIG. 3. Group data showing the effect of thalamic neuromodulators on barrel cortex single units. *A*: mean ± SE values of regular-spiking (RS) firing rate during control, CA in VPM, and NE in VPM. *B*: plot of cortical depth of RS cells as a function of the effect that CA in VPM had on firing rate: 100% means that the firing rate was not changed by CA in VPM. A linear regression fitting the data is plotted. *C*: mean ± SE values of fast-spiking (FS) firing rate during control, CA in VPM, and NE in VPM. $*P < 0.01$.

lamic spindle oscillations quite effectively during control (see *insets* in Fig. 4*A*), all of which are defining features of layer 4 FS cells (Bruno and Simons 2002; Swadlow 1995). During activation produced by application of CA in VPM, this cell stopped producing high-frequency bursts (>100 Hz) and fired almost continuously in the range of 20–50 Hz, as demonstrated by the IETH (Fig. 4*A*), an effect that was reversed by subsequent application of NE in VPM. Figure 4, *B* and *C* shows a different FS cell (900 μm in depth) together with the continuously calculated FP power spectrum and MUA activity (as in Fig. 1). Again, during activation produced by CA in VPM, this FS cell increased its firing rate in the frequency range of about 100 Hz, as revealed by the IETH (Fig. 4*C*). The effects of activation on the FS cell were reversed by deactivation produced by NE in VPM.

Intracellular (subthreshold) correlates of activation and deactivation

The previous results indicate that cortical cells undergo significant changes during application of neuromodulators in VPM. We next studied the subthreshold (intracellular) correlates of these changes. Thus we conducted intracellular recordings from cells in layers 2–4 of barrel cortex and held them during application of CA in VPM ($n = 10$) followed by NE in VPM ($n = 4$). Based on intrinsic firing properties, the recorded cells fell in the category of RS cells with different degrees of adaptation, although some could trigger a burst of action potentials at the onset of a positive current pulse (these bursts differ from typical layer 5 bursting cells in that they do not show spike attenuation within the burst). Figure 5 shows an example of a layer 2/3 cell (580 μm in depth) during control conditions and during activation produced by application of CA in VPM. During control conditions, the cell displays large-amplitude fluctuations in V_m and up and down states that are tightly synchronized with the simultaneously recorded FP population activity (Fig. 5*A*); the V_m of this cell fluctuated between −80 and −60 mV and the up state corresponded to a sharp negativity in the FP. During application of CA in VPM, the FP showed the typical pattern of activation described earlier, concomitantly the up and down states (large V_m fluctuations) of the cell were abolished, and the V_m settled around −73 mV. The excitability of the cell, measured using current pulses injected through the recording electrode, was also affected by CA in VPM. During control conditions, a positive current pulse (0.3 nA; 500 ms) produced only few action potentials (Fig. 5*B*). However, during CA in VPM the same current pulse triggered many more action potentials, indicating that the cell was more excitable. Moreover, input resistance (R_{in}), estimated using negative current pulses (Fig. 5*C*; see METHODS), was reduced by CA in VPM, suggesting increased excitability during this state. Figure 5*C* plots V_m distributions, R_{in}, and FP power spectrum measured during three different periods consisting of the control state, the period of transition between control and CA in VPM(1), and the steady period of CA in VPM(2). During application of CA in VPM, the V_m distribution became much sharper (increased peakedness), the R_{in} was reduced by 13%, and the low-frequency FP power spectrum was strongly suppressed.

The effect of CA in VPM was tested in several cells ($n = 10$) with similar effects. Figure 6 shows population data of different measures obtained from these cells. First, to estimate the peakedness of the V_m distribution, we measured the kurtosis of the distribution during control and during CA in VPM. We found a significant increase in kurtosis during CA in VPM ($P < 0.01$; Fig. 6*A*). Second, to measure the shift in the peak V_m, we fitted each V_m distribution with a nonlinear Gaussian function to derive the peak of the distribution and then subtracted the control and CA in VPM peak values (Fig. 6*B*). A positive value indicates that the cell tended to depolarize during CA in VPM, whereas a negative value indicates that the cell tended to hyperpolarize. Most of the cells showed a positive value ($n = 5$ of 10; red in Fig. 6*B*), but two cells located in layer 4 showed a negative value ($n = 2$ of 10; green in Fig. 6*B*; an example of one of these cells is presented later in Fig. 7). Third, most of the cells had a spontaneous firing rate <1 Hz ($n = 8$ of 10) and a few fired between 5 and 10 Hz ($n = 2$ of 10). As with most of the RS single units presented earlier, these cells significantly reduced their spontaneous firing rate during activation caused by CA in VPM (70 ± 9%, $P < 0.05$; note that these cells were not FS cells). This effect occurred in unison with the suppression of up and down V_m fluctuations.

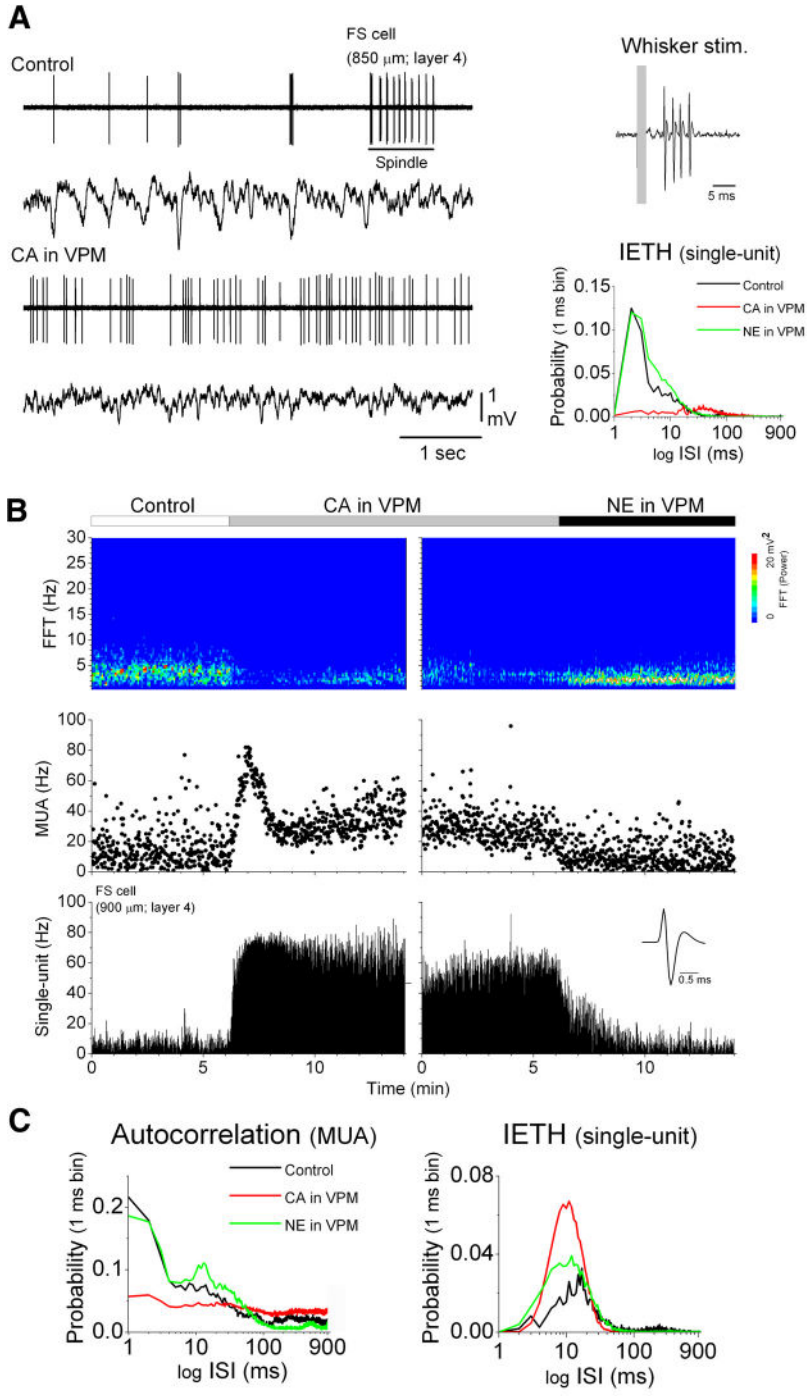

FIG. 4. Effects of thalamic neuromodulators on FS cells in barrel cortex. *A*: single-unit and FP traces showing the effect of CA in VPM on the FS cell. The *right insets* plot the response of the cell to whisker stimulation, consisting of a high-frequency burst of spikes, and an interevent time histogram (IETH) of the FS cell during control, CA in VPM, and NE in VPM. *B*: quantification of the effects of CA in VPM and subsequent NE in VPM from an experiment different from that in *A*. The *top panel* shows FFT power spectrum of the spontaneous FP activity measured continuously and displayed as a contour color plot. The *middle panel* shows the number of events detected/s (Hz) in the MUA recording measured continuously. The *bottom panel* shows the number of events detected/s (Hz) in the single-unit recording measured continuously (the *inset* shows the detected spikes). *C*: autocorrelation of the MUA and IETH of the single unit for the experiment shown in *B* during control, CA in VPM, and NE in VPM.

Thus it is important to note that the slight depolarization caused by activation in most cells did not lead to an increase in spontaneous firing rate. Finally, to measure the excitability of the cells we measured R_{in} with negative current pulses applied every 5–10 s. CA in VPM significantly suppressed R_{in} by 16.3 ± 6% ($n = 10$, $P < 0.05$; from 56 ± 10 to 46 ± 6 MΩ). In addition, it is worth noting that this measure was much more variable (CV was twice as large) during control conditions than that during CA in VPM because of the large fluctuations in V_m during control. We made no attempt to separate the effects of up and down fluctuations on R_{in} because our measurements (current pulses) were too sparse, not the high-frequency measurements required for this dissociation (Rigas and Castro-Alamancos 2009). Moreover, the effect of activation on firing triggered by positive current pulses was tested in only a few cells and thus we show only examples for those cases.

The previous results show that a few cells in layer 4 hyperpolarize during CA in VPM. Figure 7 shows an example of one of these cells (865 μm in depth). During control the cell produced up and down states and the up states triggered significant firing. CA in VPM abolished the up and down states, strongly suppressed the firing rate (Fig. 7*A*), increased the number of spikes triggered by a positive current pulse (Fig. 7*B*), and suppressed the R_{in} [CA in VPM(1); Fig. 7*C*]. However, the

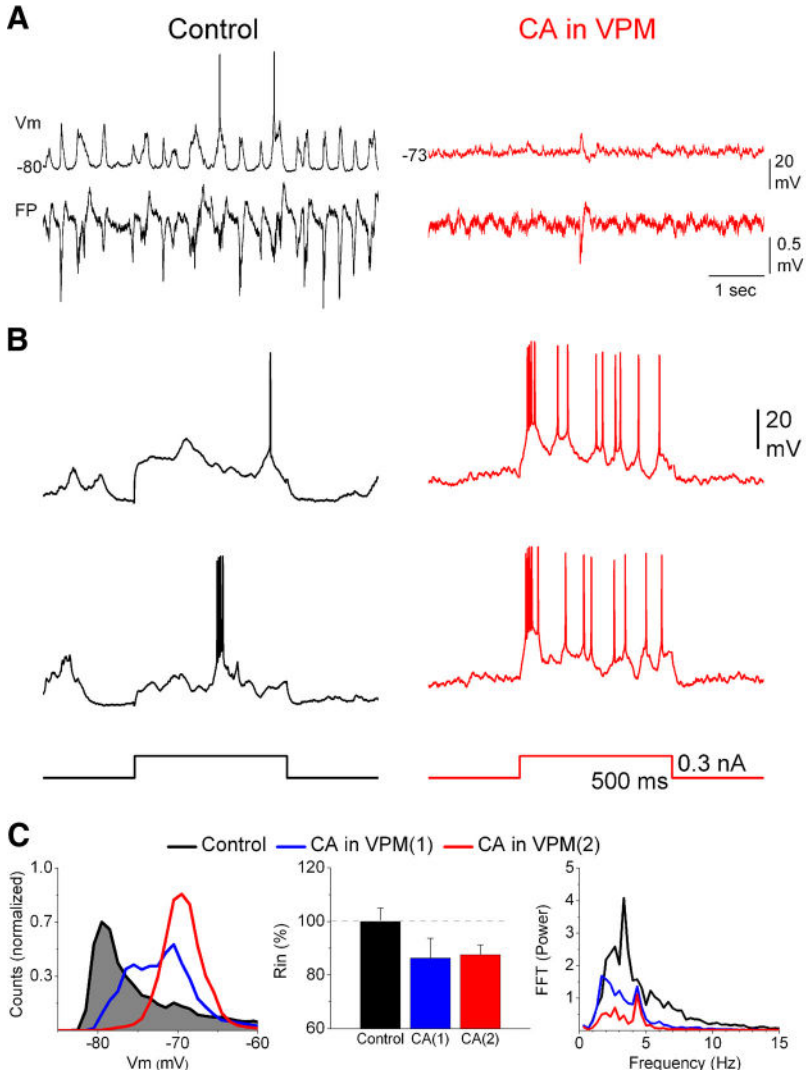

FIG. 5. Effects of thalamic CA in VPM on intracellular recordings in barrel cortex. *A*: intracellular membrane voltage (V_m) and FP traces recorded during control and during application of CA in VPM. *B*: effect of a 0.3-nA positive-current pulse (500 ms) injected into the cell during control and during CA in VPM (2 trials are shown). *C*: plots of V_m distribution, input resistance (R_{in}), and FFT FP power spectrum for the cell in *A* and *B* during control, during the transition between control and CA in VPM(1) and during the stable effect of CA in VPM(2).

cell's V_m continued to drift from −75 to −82 mV, where it stabilized, and during this state the number of action potentials evoked by a current pulse was reduced, whereas R_{in} was further suppressed [CA in VPM(2)]. These later effects on V_m, R_{in}, and firing evoked by a current pulse could be compensated by injection of constant current (+0.3 nA) into the cell [CA in VPM(3)]. One possibility is that these later changes were caused by a strong inhibitory drive in layer 4 caused by robustly firing FS cells.

As described earlier, during extracellular recordings, application of NE in VPM immediately reversed the effects of CA in VPM, producing a rapid deactivation. The same was found during intracellular recordings ($n = 4$; similar results were obtained in all these cells). Figure 8 shows an example of a cell that was impaled during CA in VPM. The cell showed the typical features of activation during this state, consisting of a sharp V_m distribution and increased excitability (measured with positive current pulses) coincident with a flat low-frequency FP power spectrum. Application of NE in VPM led to the development of large-amplitude fluctuations of the V_m (up and down states; Fig. 8*A*), which reduced the peakedness of the V_m distribution (Fig. 8*C*). There was also an apparent reduction in excitability; the positive current pulses that previously triggered many action potentials now produced fewer action potentials (Fig. 8*B*) and R_{in} increased (Fig. 8*C*; $n = 4$, $P < 0.05$). These effects were associated with an increase in the low-frequency FP power spectrum (Fig. 8*C*).

DISCUSSION

Thalamocortical cells in primary thalamic nuclei, such as VPM, are defined by their role in the relay of sensory information to the cortex. To accomplish this function, lemniscal synapses, which deliver somatosensory inputs to VPM, are very powerful (Castro-Alamancos 2002b) and drive thalamocortical cells very effectively during sensory stimulation (Castro-Alamancos 2002a, 2004b). Then, populations of thalamocortical cells discharge very tightly synchronized in response to the most effective sensory stimuli (Alonso et al. 1996; Temereanca and Simons 2003) and this synchrony is important to effectively drive cortical cells (Bruno and Sakmann 2006). In addition, thalamocortical cells can display varying states of spontaneous (i.e., nonsensory) tonic firing that is generally asynchronous (Bezdudnaya et al. 2006; Castro-Alamancos 2002a). For example, during cholinergic or noradrenergic stimulation of the thalamus, VPM cells very effectively relay sensory

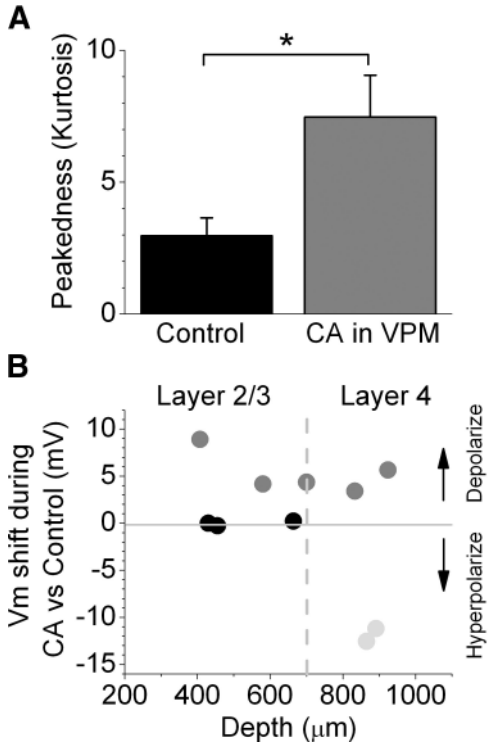

FIG. 6. Group data showing the effects of activation on the peakedness and peak shift of the V_m distribution. *A*: peakedness (kurtosis) of the V_m distribution (means ± SE) during control and during CA in VPM. *$P < 0.01$. *B*: V_m peak shift during CA in VPM as a function of depth. Cells that did not show a shift in peak are black, those that depolarized are gray, and those that hyperpolarized are light gray.

inputs to the neocortex, although the spontaneous firing of thalamocortical cells is very different in these two states—firing is robust during cholinergic stimulation and nil during noradrenergic stimulation (Hirata et al. 2006). Here we demonstrate that the different spontaneous thalamocortical firing rates, during two similarly effective sensory relay states, lead to distinct neocortex network states. The robust thalamocortical tonic firing during thalamic cholinergic stimulation produces cortical activation, whereas the nil firing during noradrenergic stimulation leads to cortical deactivation. Thus the tonic firing rate of thalamocortical cells serves to control the state of network activation in sensory cortex and this is independent of the sensory relay function of the thalamus.

Cortical activation or desynchronization (the term "desynchronized" is used traditionally but should be avoided because cells can be tightly synchronized during activation) is known to be produced by the direct effects of widespread projections originating in three main loci: the brain stem reticular formation, the intralaminar thalamic nuclei, and the basal forebrain—also known as nonspecific activating systems (e.g., Jones 1993; Vanderwolf 1988). In the present study, we bypassed stimulation of these nuclei by directly infusing drugs into the somatosensory thalamus and found that cortical activation can be controlled by thalamocortical tonic firing per se, without the need of cortically released neuromodulators originating in the traditional nonspecific systems. Therefore during some states, activity in brain stem nuclei projecting to somatosensory thalamus (see preceding text) affects thalamocortical firing, which leads to changes in cortical activation. Yet, during other conditions, basal forebrain, intralaminar nuclei, and direct brain stem projections to the cortex may produce cortical activation themselves. In relation to the potential engagement of these nonspecific systems in our study, it is important to mention that in a recent study, using thalamocortical slices, we found that thalamocortical activity per se, driven by glutamate puffs in the somatosensory thalamus, triggered or enhanced up states recorded from the barrel cortex (Rigas and Castro-Alamancos 2007). Basically, thalamocortical activity per se triggered activity resembling cortical activation (see Fig. 9 in Rigas and Castro-Alamancos 2007). The lack of stimulation of intralaminar, basal forebrain, or brain stem inputs in that experimental setup further supports the conclusion that VPM thalamocortical activity per se drives cortical activation.

In this study, we controlled thalamocortical activity by the interplay between acetylcholine and norepinephrine in the

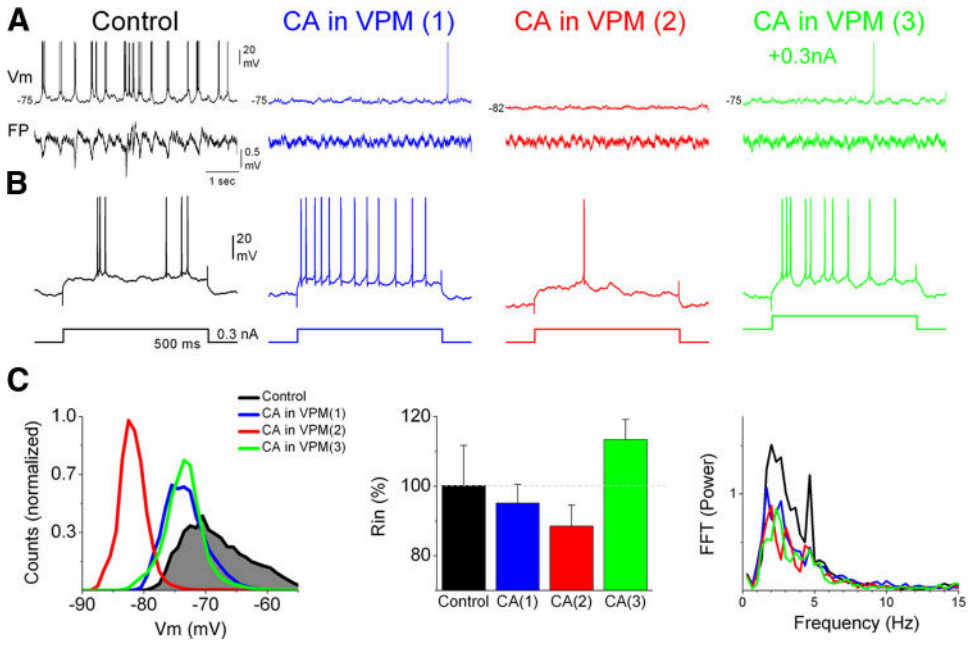

FIG. 7. Example of a cell that hyperpolarized during CA in VPM. *A*: intracellular (V_m) and FP traces recorded during control and during application of CA in VPM. The first period (1) corresponds to the initial effect of CA in VPM, the second period (2) corresponds to when the cell hyperpolarized, and the third period (3) corresponds to the injection of 0.3 nA of positive current to compensate the hyperpolarization. *B*: effect of a 0.3-nA positive-current pulse (500 ms) injected into the cell during the periods in *A* (one trial is shown). *C*: plots of V_m distribution, R_{in}, and FFT FP power spectrum for the cell in *A* and *B* during the same periods.

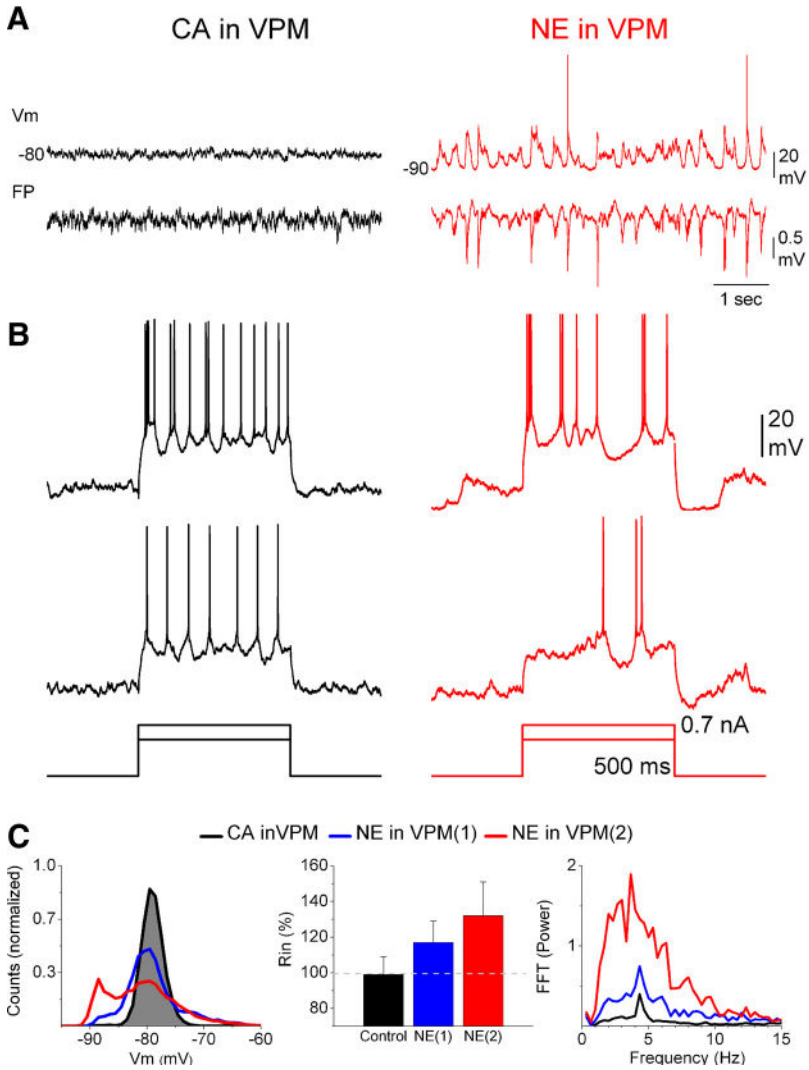

FIG. 8. Effects of thalamic NE in VPM on intracellular recordings in barrel cortex. *A*: intracellular (V_m) and FP traces recorded during CA in VPM and during application of NE in VPM. *B*: effect of 0.5- and 0.7-nA positive-current pulses (500 ms) injected into the cell during CA in VPM and during NE in VPM. *C*: plots of V_m distribution, R_{in}, and FFT FP power spectrum for the cell in *A* and *B* during CA in VPM, during the transition between CA in VPM and NE in VPM(1), and during the stable effect of NE in VPM(2).

thalamus. This raises the question of when the thalamus is influenced by acetylcholine and/or by norepinephrine. The relative levels of these neuromodulators in the thalamus during different behavioral states are not known. Also, the firing of cholinergic and noradrenergic neurons projecting to the thalamus has not been compared during different behavioral states in the same animals. However, as mentioned in the INTRODUCTION, it is known that cholinergic neurons in the LDT/PPT complex discharge vigorously during paradoxical sleep, whereas noradrenergic neurons are silent during this state. Thus the thalamus may be under cholinergic influence during paradoxical sleep, which may lead to the cortical activation typical of that state. Clearly, additional work is needed to tease apart the relative influence of these neuromodulators during different behavioral states. It will also be important to differentiate between the influences of these neuromodulators within the thalamus and within the cortex. In other words, it will be useful to determine when the thalamocortical mechanism of producing cortical activation shown here and the other established mechanisms (i.e., basal forebrain, intralaminar, brain stem reticular formation) may come into play.

Alternatively, one may simply consider the drugs used here (CA and NE) as an experimental means to change the firing rate of thalamocortical cells. In that case, the conclusions may have farther reaching consequences because any change in thalamocortical firing rate, regardless of the influence that triggers it, will serve to control the level of cortical activation. For example, the suppressing effect of NE on thalamocortical firing is mediated by nRt firing, which can be controlled by other influences. Thus thalamocortical cells can potentially change their firing rates due to many factors and thalamocortical firing controls cortical activation and deactivation.

Characteristics of neocortex activation

Stimulation in the brain stem reticular formation during surgical anesthesia is well known to produce neocortex activation resembling that observed in behaving animals (Castro-Alamancos and Oldford 2002; Moruzzi and Magoun 1949). Typically, reticular formation stimulation increases the spontaneous firing rate of VPM cells as it triggers cortical activation and reduces the spontaneous firing rate of most cells in the barrel cortex, while enhancing the firing rate of a minority of other cells (Castro-Alamancos and Oldford 2002). Although the effects of brain stem electrical stimulation are obviously much more complex than those produced by selective infusions in the thalamus, neocortex activation produced by cholinergic stimulation in the thalamus also resulted in a reduction of

spontaneous firing rate for most RS cortical cells, which was related to the abolishment of up/down V_m fluctuations. In contrast, FS cells in layer 4 robustly increased their firing rate. FS cells are well known to be tightly coupled to thalamocortical cells (Swadlow 1995); accordingly, an increase in VPM cell firing should lead to an increase in layer 4 FS cell firing.

As mentioned, during activation caused by cholinergic stimulation of the thalamus, the large-amplitude up/down V_m fluctuations of cortical cells are abolished. However, during activation, the V_m of cortical cells does not simply drift to the V_m of the up state or even more depolarized toward the reversal potential of excitatory inputs (~0 mV), as would be expected if only thalamocortical (excitatory) synapses were being stimulated in neocortex. Instead, thalamocortical synapses very effectively drive FS inhibitory neurons in layer 4 and a balance between excitation and inhibition must be reached (Okun and Lampl 2008; Shu et al. 2003). The large increase in VPM thalamocortical firing rate is correlated with a similar increase in layer 4 FS cells to avoid the runaway excitation that would otherwise occur in the barrel cortex (Okun and Lampl 2008). In our study, most cells either did not change their peak V_m or slightly depolarized without reaching the up state V_m. This suggests that the excitatory drive from thalamocortical and intracortical synapses was effectively countered by the inhibitory drive from FS cells. In addition, a few cells in layer 4 displayed a robust hyperpolarization toward the reversal potential of inhibition (between −75 and −95 mV for Cl^- and K^+), which may have been caused by a stronger inhibitory drive in these cells or other intrinsic mechanisms.

Functional role

Our findings show that thalamocortical firing per se produces cortical activation. This seems to add an additional complexity to the way cortical activation is generated, which raises the question: Why an additional mechanism? We think that cortical activation produced by thalamocortical firing is quite useful because primary thalamic nuclei, unlike nonspecific activating systems, are rather specific. The projections from these primary thalamic nuclei target very specific cortical territories and are thus capable of producing area-restricted activation that may be useful for modality-specific selective sensory processing related to selective attention demands. This would be rather difficult to accomplish with nonspecific systems because of their generally widespread projections. Thus cortical activation and deactivation controlled by thalamocortical activity may serve to control the level of activation in an area-specific manner. Furthermore, the electrophysiological signs of neocortex activation produced by CA in VPM resemble the pattern of activity observed in barrel cortex when an animal is very alert performing a sensory detection task, although this pattern can become deactivated when the animal becomes proficient in the task (Castro-Alamancos 2004a). Thus it seems feasible to conceive a neuromodulatory control system in the sensory thalamus that would allow for a rapid and selective control of neocortical activation/deactivation states as a function of modality-specific behavioral demands.

GRANTS

This work was supported by the National Institutes of Health.

REFERENCES

Aguilar JR, Castro-Alamancos MA. Spatiotemporal gating of sensory inputs in thalamus during quiescent and activated states. *J Neurosci* 25: 10990–11002, 2005.

Alonso JM, Usrey WM, Reid RC. Precisely correlated firing in cells of the lateral geniculate nucleus. *Nature* 383: 815–819, 1996.

Aston-Jones G, Bloom FE. Nonrepinephrine-containing locus coeruleus neurons in behaving rats exhibit pronounced responses to non-noxious environmental stimuli. *J Neurosci* 1: 887–900, 1981.

Bezdudnaya T, Cano M, Bereshpolova Y, Stoelzel CR, Alonso JM, Swadlow HA. Thalamic burst mode and inattention in the awake LGNd. *Neuron* 49: 421–432, 2006.

Bruno RM, Sakmann B. Cortex is driven by weak but synchronously active thalamocortical synapses. *Science* 312: 1622–1627, 2006.

Bruno RM, Simons DJ. Feedforward mechanisms of excitatory and inhibitory cortical receptive fields. *J Neurosci* 22: 10966–10975, 2002.

Castro-Alamancos MA. Origin of synchronized oscillations induced by neocortical disinhibition in vivo. *J Neurosci* 20: 9195–9206, 2000.

Castro-Alamancos MA. Different temporal processing of sensory inputs in the rat thalamus during quiescent and information processing states in vivo. *J Physiol* 539: 567–578, 2002a.

Castro-Alamancos MA. Properties of primary sensory (lemniscal) synapses in the ventrobasal thalamus and the relay of high-frequency sensory inputs. *J Neurophysiol* 87: 946–953, 2002b.

Castro-Alamancos MA. Absence of rapid sensory adaptation in neocortex during information processing states. *Neuron* 41: 455–464, 2004a.

Castro-Alamancos MA. Dynamics of sensory thalamocortical synaptic networks during information processing states. *Prog Neurobiol* 74: 213–247, 2004b.

Castro-Alamancos MA. Cortical up and activated states: implications for sensory information processing. *Neuroscientist* 15: 625–634, 2009.

Castro-Alamancos MA, Calcagnotto ME. High-pass filtering of corticothalamic activity by neuromodulators released in the thalamus during arousal: in vitro and in vivo. *J Neurophysiol* 85: 1489–1497, 2001.

Castro-Alamancos MA, Connors BW. Thalamocortical synapses. *Prog Neurobiol* 51: 581–606, 1997.

Castro-Alamancos MA, Oldford E. Cortical sensory suppression during arousal is due to the activity-dependent depression of thalamocortical synapses. *J Physiol* 541: 319–331, 2002.

el Mansari M, Sakai K, Jouvet M. Unitary characteristics of presumptive cholinergic tegmental neurons during the sleep–waking cycle in freely moving cats. *Exp Brain Res* 76: 519–529, 1989.

Foote SL, Aston-Jones G, Bloom FE. Impulse activity of locus coeruleus neurons in awake rats and monkeys is a function of sensory stimulation and arousal. *Proc Natl Acad Sci USA* 77: 3033–3037, 1980.

Guido W, Weyand T. Burst responses in thalamic relay cells of the awake behaving cat. *J Neurophysiol* 74: 1782–1786, 1995.

Hallanger AE, Levey AI, Lee HJ, Rye DB, Wainer BH. The origins of cholinergic and other subcortical afferents to the thalamus in the rat. *J Comp Neurol* 262: 105–124, 1987.

Hirata A, Aguilar J, Castro-Alamancos MA. Noradrenergic activation amplifies bottom-up and top-down signal-to-noise ratios in sensory thalamus. *J Neurosci* 26: 4426–4436, 2006.

Hirata A, Castro-Alamancos MA. Relief of synaptic depression produces long-term enhancement in thalamocortical networks. *J Neurophysiol* 95: 2479–2491, 2006.

Hirata A, Castro-Alamancos MA. Cortical transformation of wide-field (multiwhisker) sensory responses. *J Neurophysiol* 100: 358–370, 2008.

Hobson JA, McCarley RW, Wyzinski PW. Sleep cycle oscillation: reciprocal discharge by two brainstem neuronal groups. *Science* 189: 55–58, 1975.

Jones BE. The organization of central cholinergic systems and their functional importance in sleep–waking states. *Prog Brain Res* 98: 61–71, 1993.

Lindvall O, Bjorklund A, Nobin A, Stenevi U. The adrenergic innervation of the rat thalamus as revealed by the glyoxylic acid fluorescence method. *J Comp Neurol* 154: 317–347, 1974.

Moruzzi G, Magoun HW. Brain stem reticular formation and activation of the EEG. *Electroencephalogr Clin Neurophysiol* 1: 455–473, 1949.

Okun M, Lampl I. Instantaneous correlation of excitation and inhibition during ongoing and sensory-evoked activities. *Nat Neurosci* 11: 535–537, 2008.

Paxinos G, Watson C. *The Rat Brain in Stereotaxic Coordinates*. New York: Academic Press, 1982.

Rigas P, Castro-Alamancos MA. Thalamocortical up states: differential effects of intrinsic and extrinsic cortical inputs on persistent activity. *J Neurosci* 27: 4261–4272, 2007.

Rigas P, Castro-Alamancos MA. Impact of persistent cortical activity (up states) on intracortical and thalamocortical synaptic inputs. *J Neurophysiol* 102: 119–131, 2009.

Satoh K, Fibiger HC. Cholinergic neurons of the laterodorsal tegmental nucleus: efferent and afferent connections. *J Comp Neurol* 253: 277–302, 1986.

Sherman SM, Guillery RW. Functional organization of thalamocortical relays. *J Neurophysiol* 76: 1367–1395, 1996.

Shu Y, Hasenstaub A, McCormick DA. Turning on and off recurrent balanced cortical activity. *Nature* 423: 288–293, 2003.

Steriade M, Datta S, Paré D, Oakson G, Curro Dossi RC. Neuronal activities in brain-stem cholinergic nuclei related to tonic activation processes in thalamocortical systems. *J Neurosci* 10: 2541–2559, 1990.

Steriade M, Dossi RC, Nunez A. Network modulation of a slow intrinsic oscillation of cat thalamocortical neurons implicated in sleep delta waves: cortically induced synchronization and brainstem cholinergic suppression. *J Neurosci* 11: 3200–3217, 1991.

Steriade M, Jones EG, McCormick DA. *Thalamus.* New York: Elsevier, 1997.

Swadlow HA. Influence of VPM afferents on putative inhibitory interneurons in S1 of the awake rabbit: evidence from cross-correlation, microstimulation, and latencies to peripheral sensory stimulation. *J Neurophysiol* 73: 1584–1599, 1995.

Temereanca S, Simons DJ. Local field potentials and the encoding of whisker deflections by population firing synchrony in thalamic barreloids. *J Neurophysiol* 89: 2137–2145, 2003.

Vanderwolf CH. Cerebral activity and behavior: control by central cholinergic and serotonergic systems. *Int Rev Neurobiol* 30: 225–340, 1988.

Williams JA, Comisarow J, Day J, Fibiger HC, Reiner PB. State-dependent release of acetylcholine in rat thalamus measured by in vivo microdialysis. *J Neurosci* 14: 5236–5242, 1994.